Available online at www.sciencedirect.com

ScienceDirect

Energy Procedia 101 (2016) 528 – 535

Energy Procedia

71st Conference of the Italian Thermal Machines Engineering Association, ATI2016, 14-16 September 2016, Turin, Italy

Analysis of an integrated agro-waste gasification and 120 kW SOFC CHP system: modeling and experimental investigation

Antonio Galvagno[a]*, Mauro Prestipino[a], Giovanni Zafarana[b] and Vitaliano Chiodo[b].

[a] *University of Messina, Department of Engineering, C.da Di Dio (Vill.S.Agata), Messina – 98158, Italy*
[b] *Institute CNR – ITAE, via Salita Santa Lucia sopra Contesse 5, Messina – 98126, Italy*

Abstract

Renewable sources of hydrogen are of major interest in the context of energy production through fuel cells. The technical feasibility of CHP system composed by orange peels steam/air gasification unit coupled with a solid oxide fuel cell (SOFC) was investigated in this study. To this purpose, a zero-dimensional process simulation model of the CHP system using Aspen Plus was developed. Mathematical model was experimentally validated in a lab scale apparatus. Moreover, optimal operative conditions and integration options were investigated, as well as the system maximum theoretical overall efficiency. Results showed that in order to obtain 120 kW of DC power from the specific SOFC, 65 kg/h of biomass with 20% of moisture and 173 kg/h of raw biomass with 70% of water needed to be fed in the CHP system. It was theoretically proved that 120 kW of DC power and 135 kW of heat could be produced from SOFC unit at the selected operative conditions, with a net CHP maximum efficiency equal to 74%.

Peer-review under responsibility of the Scientific Committee of ATI 2016.

Keywords: biomass gasification; SOFC; citrus peels; combined heat and power; software simulation; ASPEN plus;

1. Introduction

During the most recent years, biomass is playing a relevant role among the different forms of renewable energy sources. While energy has become a central topic of the worldwide political agenda, many countries, including Italy, have introduced important incentives to support the use of biomass to produce electricity and heat. This has raised

* Corresponding author. Tel.: +39-090-3977564
E-mail address: agalvagno@unime.it

Peer-review under responsibility of the Scientific Committee of ATI 2016.
doi:10.1016/j.egypro.2016.11.067

considerable interest towards the use of biomass for energy production [1-2]. Although the energy valorization of agro-industrial waste can reduce fossil fuel dependency and greenhouse gas (GHG) emissions [3–4], they are not properly exploited [5]. In particular, Italian citrus industry consumes about 3.8 million tons of fruits (mainly oranges and lemons) produced in a cultivated area of about 160,000 ha [6]. Sicily is one of the largest citrus producer among the Italian regions. Its share of annual production is about 1.25 million tons of oranges (51% of Italian total production) and 0.45 million tons of lemons (87% of the national production) many of which are used to produce citrus fruit juice [7]. Every year in Italy, the juice industries process about 1.5 million tons of citrus fruit and 1 million tons of citrus peel waste are produced, involving significant environmental problem related to disposal of solid wastes [8]. In fact, orange peel waste (OPW), the solid residue from the orange juice extraction process consisting of peel, rag (segment membranes and cores), juice sacs, and seeds, amounts to 50–70% of the fresh fruit mass [9]. In the OPW most of the weight consists of water (over 80%). For this reason, interest in alternative uses of these by-products attracts the research community. Several thermochemical (e.g., pyrolysis, gasification, liquefaction, hydrothermal conversion and torrefaction) and biochemical (e.g., enzymatic hydrolysis and fermentation) technologies are available to convert this biomass to biofuels, such as bio-oils, synthesis gas (or syngas) and ethanol [10-13].

Gasification process converts biomass through partial oxidation into a gaseous mixture of syngas consisting of hydrogen (H_2), carbon monoxide (CO), methane (CH_4) and carbon dioxide (CO_2). The oxidant or gasifying agents can be air, pure O_2, steam, CO_2 or their mixtures. Air, while a cheap and widely used gasifying agent contains a large amount of nitrogen, which lowers the heating value of the produced syngas. The heating value and H_2 content of syngas could be increased by addiction of steam in the inlet gas stream as gasifying agent. Alternatively, a mixture of steam or CO_2 and air or O_2 can be used as gasifying agent, and the partial combustion of biomass with air/O_2 provides the heat required for the gasification [14]. Operative conditions and syngas composition of the gasification process make it attractive in combined heat and power generation systems with high temperature fuel cell like SOFC.

The aim of this work was to investigate the technical feasibility of a CHP system, where a solid oxide fuel cell system has been combined with an orange peels gasificator (using air and steam as oxidant). A zero-dimensional simulation model, using Aspen Plus simulator, was used to analyze the combined system. Mathematical model of the gasification unit was experimentally validated by lab-scale experiments, while the SOFC model was validated with data available in literature. After the stand-alone models validation, the two unit models were integrated in order to simulate the syngas production process combined with the syngas utilization through a SOFC unit. Moreover, optimal operative conditions and integration options were investigated and maximum theoretical overall efficiency of the system was calculated.

2. Mathematical models and methods

An Aspen Plus simulation model was developed with the aim of simulating a theoretical gasification process. The mathematical model was used in order to calculate the amount of feedstock that it is necessary to produce the syngas required by a 120 kW DC SOFC unit. The integrated simulation model, showed in Figure 1, is divided in three main sections, which represent three different units: biomass dryer, gasification process and SOFC. The first section describes the feedstock drying that occurs outside the gasification reactor. Since the OPW can be mechanically dried up to 70%$_{wt/wt}$ of water content, it was necessary to use a thermal dryer in order to reach 20%$_{wt/wt}$ of moisture content, which is the maximum limit for the gasification process. The exhaust heat from the SOFC unit provides the required heat for the dryer. The specific drying heat ("Q_{dry}" in kJ/kg) was calculated according the following equation:

$$Q_{dry} = \left[c_{p-biom} \cdot DM \cdot \Delta T_1 + c_{p-H2O} \cdot (1 - DM) \cdot \Delta T_2 + (h_{383v} - h_{373l}) \cdot x_{ev}\right] / \eta_{dry} \quad (1)$$

where $c_{p\text{-}biom}$ and $c_{p\text{-}H2O}$ are the specific heat [kJ/kgK] of dry biomass and water, respectively, while DM is the dry matter fraction [wt/wt]; ΔT_1 (110 K) and ΔT_2 (90 K), are the temperature variations from room temperature (283 K) for solid and the water fraction in the wet biomass, respectively; h_{383v} and h_{373l} are the steam enthalpy at 383 K and the one of water at 373 K [kJ/kg], x_{ev} is the evaporated water fraction of the original wet biomass. A typical dryer efficiency, η_{dry} , was also considered (about 70% [15]). In the second section, the gasification unit is simulated, where biomass is first completely dried inside the reactor and then subjected to the pyrolysis, gasification and combustion steps. With regard to the pyrolysis one, the gasification model proposed in this work is founded on a semi-regressive approach based on the biomass decomposition in tar, char and gas, according to the experimental yields obtained

during pyrolysis laboratory tests. The decomposition products, along with the gasifying agents (air and steam mix), are entirely directed into a Gibbs reactor at 1073 K, which models the gasification steps and where all chemical components participate in possible reactions and the output stream is calculated minimizing the Gibbs free energy.

The model was run using different steam to biomass ratios (S/B = 1; 1.5 and $2_{wt/wt}$) and fixing the equivalence ratio (ER= process air/stoichiometric air) at 0.35. After the gasification block (GASIFIC), syngas is cooled using two heat exchangers. The first one was used to produce steam for the gasification reactor (COOLER1 block). While in the second one (COOLER2 block) the syngas temperature is lowered until the steam molar percentage in the syngas stream reached the desired value for the SOFC operation (about $12\%_{(vol/vol)}$). The water molar fraction in the syngas stream is optimized by maximizing the hydrogen partial pressure in the reformed syngas (REFSYNG stream in SOFC unit). The main reforming reactions (water-gas shift and steam reforming) occur in the PREREFOR block.

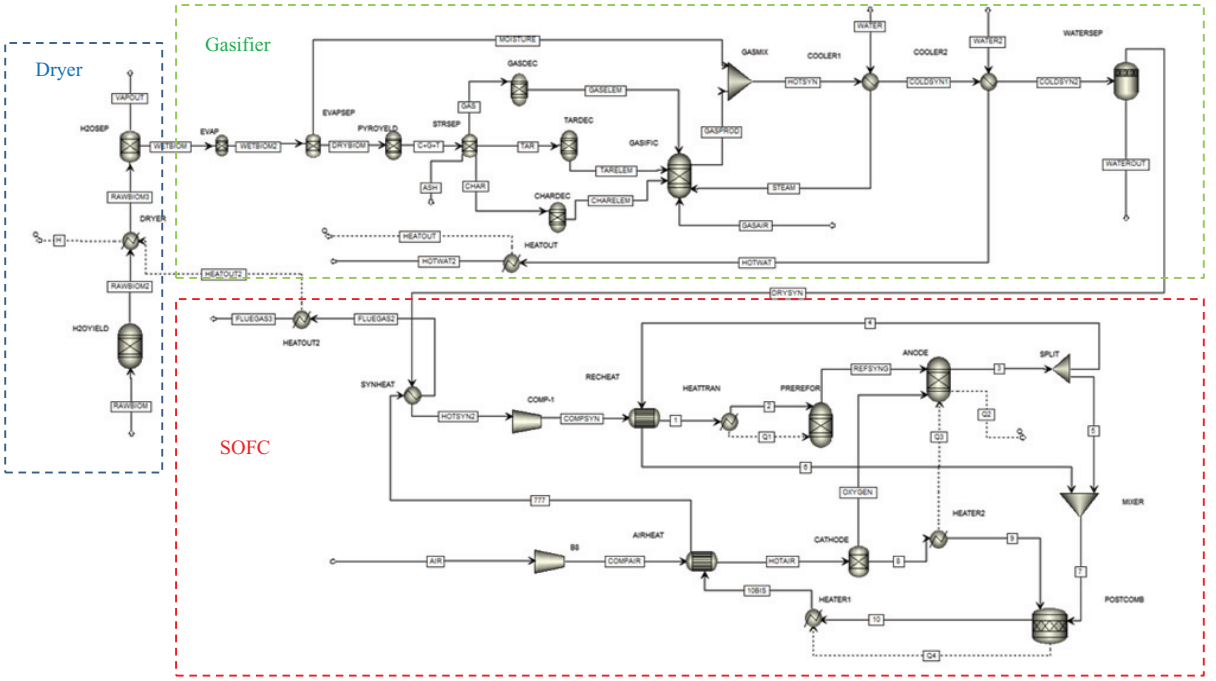

Fig. 1 Simulation model of integrated citrus peel drying unit, gasification unit and SOFC unit.

The third section of the simulation model describes a SOFC tubular fuel cell developed by SIEMENS that it is based on a typical scheme used in literature by several authors [16-19]. In this study, the SOFC unit design was optimized in order to maximize the heat production from the stack. In ASPEN plus environment it is not possible to model the semi reactions, the ion crossover and the electrons migrations, thus the overall reaction of water formation from H_2 and O_2 is modeled in the ANODE block. In the CATHODE block the oxygen is separated and directed to the anode in order to reach the require amount for the reactions. The amount of oxygen split into the anode is calculated on the base of the fuel utilization factor (U_f), i.e. the ratio between the hydrogen consumed in the reaction and the hydrogen flow rate in the syngas (typically 0.85), as reported in the following equations:

$$nH_{2,in} = nH_{2,syngas} + nCO_{syngas} + 4nCH_{4,syngas} \quad (2)$$

$$U_f = \frac{nH_{2,consumed}}{nH_{2,in}} \quad (3)$$

$$nO_{2,consumed} = 0.5\, nH_{2,consumed} \quad (4)$$

$$O_{2,split} = \frac{nO_{2,consumed}}{nO_{2,in}} \quad (5)$$

where nX_{in}, nX_{syngas}, $nX_{consumed}$ and $O_{2,\ split}$ are the molar flows [kmol/h] of the chemical species that are fed in the SOFC unit, the molar flows in the syngas stream, the consumed molar flows in the SOFC unit and the oxygen molar fraction that is split from the cathode to the anode, respectively.

The voltage calculation, obtained as function of current density, j (mA/cm^2), was performed applying the Nernst equation, in order to obtain the Nernst potential (V_N), and subtracting voltage losses, which comprise Ohmic (V_{Ohm}), Activation (V_a) and Concentration losses (V_c), the cell voltage can be obtained as follow:

$$V = V_N - V_{Ohm} - V_a - V_C = V_N - \left(V_{Ohm_A} + V_{Ohm_C} + V_{Ohm_E} + V_{Ohm_{Int}}\right) - j \cdot \left(R_{act_A} + R_{act_C}\right) - \left(V_{conc_A} + V_{conc_C}\right) \quad (6)$$

The terms of the above equations, related to voltage losses, were calculated according to equations available in literature for these tubular SOFC systems [18-22], which are shown in Table1.

Table 1 Voltage Loss equations [18]

Ohmic loss	
Anode	$V_{Ohm\_A} = \frac{j \cdot \rho_A (A \cdot \pi \cdot D_m)^2}{8 \cdot t_A}$
Cathode	$V_{Ohm\_C} = \frac{j \cdot \rho_C \left(\pi \cdot D_m\right)^2}{8 \cdot t_C} \cdot A[A + 2(1 - A - B)]$
Electrolyte	$V_{Ohm\_E} = j \cdot \rho_E \cdot t_E$
Interconnection	$V_{Ohm\_Int} = j \cdot \rho_{Int} (\pi \cdot D_m) \frac{t_{Int}}{W_{Int}}$
Activation loss	
Anode	$\frac{1}{R_{act\_A}} = \frac{2 \cdot F}{R_g \cdot T_{op}} \cdot k_A \left(\frac{P_{H_2}}{T^2}\right)^m \exp\left(\frac{-E_A}{R_g \cdot T_{op}}\right)$
Cathode	$\frac{1}{R_{act\_C}} = \frac{4 \cdot F}{R_g \cdot T_{op}} \cdot k_C \left(\frac{P_{O_2}}{T^2}\right)^m \exp\left(\frac{-E_C}{R_g \cdot T_{op}}\right)$
Concentration loss	
Anode	$V_{Conc\_A} = -\frac{R_g \cdot T_{op}}{2 \cdot F} \ln\left[\frac{1 - (R_g \cdot T_{op}/2 \cdot F)(t_A / D_{An,eff}) \cdot y^0_{H_2} \cdot P_{SOFC})j}{1 + (R_g \cdot T_{op}/2 \cdot F)(t_A / D_{An,eff}) \cdot y^0_{H_2O} \cdot P_{SOFC})j}\right]$
Cathode	$V_{Conc\_C} = -\frac{R_g \cdot T_{op}}{4 \cdot F} \ln\left\{\frac{(P_{SOFC}/\delta_{O_2}) - [(P_{SOFC}/\delta_{O_2}) - y^0_{O_2} \cdot P_{SOFC}] \exp[(R_g \cdot T_{op}/4 \cdot F)(\delta_{O_2} \cdot t_C / D_{Cat,eff}) \cdot P_{SOFC})j]}{y^0_{O_2} \cdot P_{SOFC}}\right\}$

Doherty et al. [18] showed the details of fuel cell parameters shown in Table 1, such as geometry, material properties, ohmic losses, activation losses and concentration losses that have to be used for voltage calculations. The electrical operating conditions of the SOFC unit, such as current density and cell voltage, were determine through the evaluation of the polarization, power density and gross AC efficiency curves (Figure 3). The ASPEN plus software was used for the mass and heat streams calculations. For the syngas flow rate calculation, at first it was necessary to know the cell active area, in order to obtain the cell current (I). This was evaluated considering 96.0768 m^2 for 1152 cells [18,19] (0.0834 m^2/cell) allowing the cell current determination for a fixed current density. Then it was possible to calculate the actual cells number for the desired DC Power stack (120 kW). Consequently the hydrogen molar flow rate ($nH_{2,in}$) and the fuel molar flow rate ($nFuel_{in}$) were calculated as follow:

$$n_{H_2,in} = \frac{I \times 3600}{2FU_f \times 1000} \quad (7)$$

$$nFuel_{in} = \frac{n_{H_2,in}}{x_{H_2} + x_{CO} + 4 \cdot x_{CH_4}} \quad (8)$$

where $n_{H_2,in}$ and $nFuel_{in}$ are expressed in kmol/s, while F and x are the Faraday constant (C/mol) and the molar fraction of gaseous components, respectively. Then, the gasification and SOFC models were integrated in order to determine the biomass feeding rate that is necessary for producing the syngas amount that has to be fed in the 120 kW DC SOFC unit. This calculation has been done through a design specification block, which allowed the determination of biomass feeding rate after fixing the syngas flow rate output.

The SOFC and CHP plant net efficiency were calculated as follows:

$$\eta_{SOFC,net} = \frac{P_{AC}}{\dot{m}_{syn} \cdot LHV_{syn}} \quad (9)$$

$$\eta_{CHP,net} = \frac{(P_{AC} - P_{el,int}) + (Q_{SOFC} + Q_{syn} - Q_{dry})}{(\dot{m}_{biom} \cdot LHV_{biom})} \quad (10)$$

where $\dot{m}_{syn}$, $\dot{m}_{biom}$, LHV_{syn} and LHV_{biom} are syngas flow rate (kg/s) of the DRYSYN stream, biomass (WETBIOM stream with 20% of water content) feeding flow rate (kg/s), syngas and biomass lower heating values, respectively. While P_{AC} is the SOFC AC power output, $P_{el,int}$ is the internal power consumption, Q_{SOFC} is the maximum recoverable heat from the SOFC, Q_{syn} is the maximum recoverable heat from syngas cooling (COOLER2) and Q_{dry} is the required heat to dry the syngas up to 20% of water content.

2.1. Experimental apparatus and procedures

Experiments were carried out at atmospheric pressure in a fixed bed stainless steel reactor (h=600 mm; i.d. =12 mm) equipped with a mobile furnace. About 3 g of orange peels were packed in a reactor zone placed outside of the furnace and purged with argon. The furnace is moved toward biomass bed only after getting the operative temperature (1073 K), then steam/air mix was purged inside the reactor. The orange peels were preventively air dried (383 K for 1 h), shredded and sieved into a grain size range of 0.7-0.4 mm. The feed flow rate of air (ER=0.35) was kept constant to 40 cc/min (STP) by mass flow meter. While the H_2O flow (S/B = 1.0-2.0$_{wt/wt}$) was fed by an isocratic HP 1100 pump and vaporized in a stainless steel reactor held at 503 K. The outlet gas stream came in through a cold trap composed by two condensers in order to obtain analyzable gas (syngas) and liquid (oil) phases. The syngas composition was qualitative and quantitative analyzed by on line GC system (Agilent HP 6890 Plus) equipped with TCD/FID detectors, while the total gas volume was measured by a flow-meter system. The citrus peel was characterized by proximate, ultimate analysis and HHV (higher heating value) as reported in Table 2. Ultimate and proximate analysis were calculated according with literature data [23]. Furthermore, thermodynamic gasification reactions were analyzed using Aspen plus software in order to calculate the outlet stream compositions promoted by air-steam citrus peel gasification.

Table 2: Characteristics of citrus peel feedstock

Ultimate Analysis (%)						
	C	H	N	S	O[a]	Ash
As received	34.3	5.0	1.0	0.1	32.6	6.9
Dry Basis	42.9	6.3	1.3	0.1	40.8	8.5
	Proximate Analysis (%)				**HHV**	**LHV**
Moisture	VM	FC	Ash		(MJ/kg)	(MJ/kg)
20.0	57.5	15.5	6.9		14.41	13.84

a. by difference

3. Experimental results and models validation

3.1. Gasification model validation

Table 3 shows experimental and theoretical data of citrus peel gasification tests, in terms of outlet stream compositions. It was observed that H_2 production increased with S/B ratio both experimental and simulation tests. Furthermore, a good match between experimental and theoretical data was recorded for all gasification runs. The decrease of the carbon monoxide with the amount of the water was attributed to the water gas shift reaction [24], that enhances the increase of the CO_2. Traces of methane were recorded during the experimental tests derived from hydro-gasification of carbon reaction ($C+2H_2 \leftrightarrow CH_4$; $\Delta H293 = -87$ kJ/mol), that is characterized by a slightly exothermic reaction, resulting in a very low concentration of CH4 in the gas stream at 1073 K.

The H_2/CO ratio is a parameter selected as a benchmark of efficiency for the purpose of syngas production from gasification process, moreover, this ratio resulted to be a basic parameter for SOFC applications [25, 26]. In this context, the H_2/CO ratio has been evaluated along with the considered S/B ratio range, as reported in Figure 2a.

Table 3: Outlet gas stream composition (dry-syngas) of the air/steam gasification experimental test conducted at 1073 K (ER: 0.35) compared with the thermodynamic data in the same operative conditions

	Experimental					Thermodynamic				
S/B	H_2	CO_2	CO	CH_4	N_2	H_2	CO_2	CO	CH_4	N_2
1.0	28.1	15.8	19.6	0.4	36.1	29.3	13.7	16.5	0.1	40.4
1.5	29.1	17.8	14.6	0.3	38.2	31.0	16.0	13.5	0.0	39.5
2.0	30.4	19.5	11.9	0.2	38.0	32.2	17.4	11.5	0.0	38.9

The highest H_2/CO ratio (2.6) was reached at the highest S/B ratio. The very near approach to the equilibrium of the H_2/CO ratio for high water concentration is probably related to the synergic participation of the main gasification reactions (water gas-shift and steam-carbon reactions) that contribute to enhance the hydrogen concentration along with the increase of the H_2/CO ratio.

3.2. SOFC stack model validation

Electrical performances of the SOFC model were validated with data available in literature [18]. Figure 2b shows the comparison between the polarization curve obtained by Doherty et al. [18] and the one obtained in this work, using the same operating conditions, cell parameters and syngas composition. The results show a good agreement between the Doherty model and the replicated one.

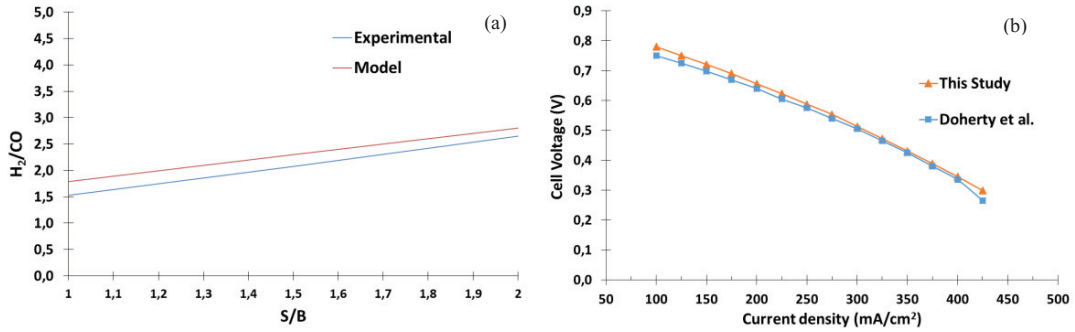

Fig. 2: Gasification model (a) and SOFC model (b) validation.

4. Integrated model simulation results

After the standalone models validation, the simulation models were run using the actual syngas composition shown in table 3 at S/B= 2 and ER = 0.35, which presented the highest H_2 concentration among the investigated conditions. The optimized water content in the syngas that is entering in the SOFC unit, was calculated using an "optimization block" in Aspen Plus, setting as target the H_2 partial pressure maximization in the anode inlet stream. In fact, as mentioned before, the SOFC unit is provided by a pre-reformer block, where steam reforming and water gas shift reaction take place. Figure 3 shows the effect of current density on DC power density (mW/cm^2), cell voltage (mV) and AC efficiency (%). It is well established that there must be a trade-off between current density, power density and efficiency, that imply a compromise between capital and operating costs [18,19]. As it is possible to infer from the AC efficiency trend, that has been calculated based on syngas LHV, the cell efficiency decrease from 0.56 to 0.16, as the current density increase from 100 to 475 mA/cm^2. Typical values of current density, for this type of fuel cells, are from 150 to 300 mA/cm^2 [18,19]. In this study, a current density of 200 mA/cm^2 was considered, corresponding to

cell voltage and DC power density values of 0.740 V and 148 mW/cm^2, respectively.

The SOFC unit was operated under the above mentioned conditions and the required amount of syngas was calculated according to equations (7) and (8).

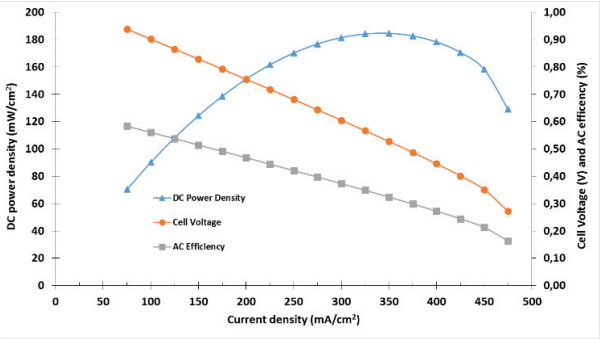

Figure 3: Effect of current density on cell voltage and DC power density.

Simulation results showed that it is necessary as much as 9.09 kmol/h of syngas to produce 200 mA/cm^2. The two models were integrated and the gasification unit model was also equipped with a "design specification block" (available in Aspen Plus) in order to determine the biomass feeding rate that was necessary for the specified syngas flow rate. The required feedstock rate was equal to 65 kg/h and 173 kg/h for biomass with 20%$_{(wt/wt)}$ and 70%$_{(wt/wt)}$ of moisture, respectively. As explained in the mathematical model description section, the SOFC unit was mainly developed for the energy and mass balance study. Table 4 shows the effects of the current density variation from 300 mA/cm^2 (Case1) to 200 mA/cm^2 (Case 2a and 2b) and the effects of using an additional syngas preheater (Case 2a without syngas preheat and Case 2b with syngas preheat).

Table 4: Main results of the integrated simulation model

Parameter	Case 1	Case 2a	Case 2b
Current Density (mA/cm^2)	300	200	200
Cell voltage (mV)	590	740	740
Internal power consumptions (kW)	28	15	20
Net AC Power	86	99	95
SOFC AC gross efficiency (%)	37	47	47
SOFC AC net efficiency (%)	28	41	39
Biomass thermal input (kW)	312	250	250
Drying thermal input (kW)	151	125	125
Max. recoverable heat (SOFC flue gas/syngas cooling) (kW)	159/87	125/70	135/70
Plant net CHP efficiency (%, LHV basis)	58	68	70

As expected, as the current density increase from 200 to 300 mA/cm^2 the SOFC gross efficiency decrease because the voltage loss implies an higher syngas flow rate for keeping the fixed electrical power output. In addition, the increased current density involves higher internal power consumption, with a consequent drastic loss of net efficiency. In Case 2b, the additional syngas preheating from 323 to 573K, before the SOFC inlet (SYNHEAT block), implies that the recoverable heat, from the SOFC flue gas, increases from 125 to 135 kW. From Table 4 can be also observed that syngas preheating allows the net CHP efficiency to increase from 66% to 70%, because of the increased recoverable heat.

5. Conclusion

Process simulation software was employed in order to develop the feasibility study of energy production from citrus peels air/steam gasification coupled with a 120 kW (DC) SOFC unit. The gasification unit model was validated by experimental tests, while the SOFC unit model was validated from literature data. The integrated simulation model revealed that the required amount of semi-dry biomass (20% of moisture) was equal to 65 kg/h, with an energy content of 13.8 MJ/kg (LHV). This amount corresponds to 173 kg/h of raw biomass with 70% of water content, as it comes out from the juice extraction process. Different configurations of the integrated model pointed out that an additional heating step, before the fuel cell stack inlet, allows maximizing the recoverable heat from the SOFC unit and the net efficiency of the CHP plant, achieving values of 135 kW and 70%, respectively. Therefore, the energy exploitation of citrus peel from juice producers was theoretically proved through SOFC system fed by a biomass air/steam gasification unit. The feasibility study also proved that the heat produced from the fuel cell could provide the energy for the drying unit, which often represent a key issue for the citrus wastes management, making the proposed thermochemical biomass conversion process a sustainable pathway for the valorization of this kind of agro-industrial waste.

References

[1] Sanders J, Van Der Hoeven D. Opportunities for a Bio-based Economy in the Netherlands. Energies 2008;1:105–119.
[2] Koseki H. Evaluation of Various Solid Biomass Fuels Using Thermal Analysis and Gas Emission Tests. Energies 2011;4:616–627.
[3] Antolìn G, Irusta R, Velasco E, Carrasco J, Gonzàlez E, et all. Biomass as an energy resource in Castilla y Leon. Energy 1996;21:165-172.
[4] Fernandes U, Costa M. Potential of biomass residues for energy production and utilization in a region of Portugal. Biomass Bioenergy 2010;34:661–666.
[5] Messineo A, Volpe R, Asdrubali F. Evaluation of net energy obtainable from combustion of stabilised olive mill by-products, Energies 2012;5:1384–1397.
[6]Censimento ISTAT Agricoltura 2010. http://dati.istat.it/Index.aspx?DataSetCode=DCSPCOLTIVAZ/.
[7] Patto di sviluppo del distretto produttivo Agrumi di Sicilia, http://www.distrettoagrumidisicilia.it/writable/allegati/patto+sviluppo276.pdf/
[8] Volpe M, Panno D, Volpe R, Messineo A. Upgrade of citrus waste as a biofuel via slow pyrolysis. J. of Analytical and Applied Pyrolysis 2015;115:66-76.
[9] Crawshaw R. Co-product feeds: animal feeds from the food and drinks industries. Nottingham: Nottingham University Press; 2004.
[10] Nanda S, Mohammad J, Reddy SN, Kozinski JA, Dalai AK. Pathways of lignocellulosic biomass conversion to renewable fuels. Biomass Convers Bioref 2014;4:157–91.
[11] Zhang L, Xu CC, Champagne P. Overview of recent advances in thermochemical conversion of biomass. Energy Conv. and Manag. 2010;51:969–82.
[12] Nanda S, Isen J, Dalai AK, Kozinski JA. Gasification of fruit wastes and agro-food residues in supercritical water. Energy Conv. and Manag. 2016;110:296-306.
[13] Frusteri F, Italiano G, Espro C, Cannilla C, Bonura G. H 2 production by methane decomposition: Catalytic and technological aspects. Int. J. of Hydrogen Energy 2012;37:16367-74
[14] Gil J, Corella J, Aznar MP, Caballero MA. Biomass gasification in atmospheric and bubbling fluidized bed: effect of the type of gasifying agent on the product distribution. Biomass & Bioenergy 1999;17:389–403.
[15] G. Haarlemmer. Simulation study of improved biomass drying efficiency for biomass gasification plants by integration of the water gas shift section in the drying process, Biomass and Bioenergy 2015;81:129-136.
[16] Zhang W, Croiset E, Douglas PL, Fowler MW, Entchev E. Simulation of a tubular solid oxide fuel cell stack using AspenPlusTM unit operation models. Energy Conversion and Management 2005;46:181-96.
[17] Anderson T, Vijiai P, Tade M.O. An adaptable steady state Aspen Hysys model for the methane fuelled solid oxide fuel cell. Chemical Engineering Research and Design 2014;92:295–307.
[18] W. Doherty, A. Reynolds, D. Kennedy. Computer simulation of biomass gasification-solid oxide fuel cell power system using ASPEN Plus, Energy 2010;35:4545-4555.
[19] W. Doherty, A. Reynolds, D. Kennedy. Process simulation of biomass gasification integrated with a solid oxide fuel cell stack. Journal of Power Sources 2015;277:292-303.
[20] Song TW, Sohn JL, Kim JH, Kim TS, Ro ST, Suzuki K. Performance analysis of a tubular solid oxide fuel cell/micro gas turbine hybrid power system based on a quasi-two dimensional model. Journal of Power Sources 2005;142:30-42.
[21] Achenbach E. Three-dimensional and time-dependent simulation of a planar solid oxide fuel cell stack. J of Power Sources 1994;49:333-48.
[22] Chan SH, Khor KA, Xia ZT. A complete polarization model of a solid oxide fuel cell and its sensitivity to the change of cell component thickness. Journal of Power Sources 2001;93:130-40.
[23] N. Mahinpey, P. Murugan, T. Mani, R. Raina, Analysis of Bio-Oil, Biogas, and Biochar from Pressurized Pyrolysis of Wheat Straw Using a Tubular Reactor, Energy Fuels 2009;23:2736–42.
[24] L. Wei, S. Xu, J. Liu, C. Liu, S. Liu. Hydrogen Production in Steam Gasification of Biomass with CaO as a CO2 Absorbent. Energy & Fuels 2008;22:1997–2004.
[25] V. Chiodo, A. Galvagno, A. Lanzini, D. Papurello, F. Urbani, M. Sanatarelli, S. Freni. Biogas refroming process investigation for SOFC application, En. Conv. Manag. 2015;98:252-258.
[26] Z. Ravaghi-Ardebili, F. Manenti, C. Pirola, F. Soares, M. Corbetta, S. Pierucci, E. Ranzi. Influence of the Effective Parameters on H_2:CO Ratio of Syngas at Low- Temperature Gasification, Chemical Engineering Transactions 2014;37:253-258.